IEEE Access
Multidisciplinary ⋮ Rapid Review ⋮ Open Access Journal

Received 5 September 2026, accepted 10 October 2026, date of publication 19 October 2026, date of current version 23 October 2026.

Digital Object Identifier 10.1109/ACCESS.2026.3744344

RESEARCH ARTICLE

A Feasibility Study Comparing Body-Powered and Myoelectric Prostheses Using Plug-and-Play Module

RISHI ADUSUMILLI[1], SOUVIK PODDAR[1], MOHAMED SULAIMAN[1], AND JIYEON KANG[1,2], (Member, IEEE)

[1]Mechanical and Aerospace Engineering Department, University at Buffalo, Buffalo, NY 14260, USA
[2]Department of AI Convergence, Gwangju Institute of Science and Technology, Gwangju 61005, South Korea

Corresponding author: Jiyeon Kang (jkangrobot@gist.ac.kr)

This work was supported in part by Korean government's Ministry of Science and Information and Communications Technology (MSIT) through the National Research Foundation of Korea (NRF) under the (Bio and Medical Technology Development Program) under Grant RS-2024-00361688, in part by the Institute of Information and Communications Technology Planning and Evaluation (IITP) through the (AI Star Fellowship Support Program) under Grant IITP-2026-RS-2026-25615334, and in part by the InnoCORE Program under Grant KH1460 and Grant GKH1430.

ABSTRACT Two types of widely used prostheses are the body-powered prosthesis actuated with the shoulder/trunk movement and the myoelectric prosthesis actuated with a motor using sEMG signals. Even though these devices have been used for several decades, controlled quantitative comparisons that isolate the effects of prosthetic actuation strategy under identical mechanical interfaces remain limited. The challenges of the comparison studies stem from factors including different interfaces of these devices, different shape/length of the residual limb, the cause of amputation, or frequency of the prosthesis use during daily life. In this study, we designed a plug-and-play module that can change the body-powered prosthesis easily to a myoelectric prosthesis while keeping the interface structure of the body-powered prosthesis offering a cost-effective and personalized solution. Ten non-amputee participants were recruited to conduct three daily living tasks by wearing two different prostheses with a bypass of their own forearm. These participants were assumed to be novice users of both body-powered and myoelectric prostheses. The myoelectric prosthesis reduced compensatory ipsilateral elbow motion by approximately 30%, with significant reductions observed in two of the three tasks ($p < 0.001$), and contralateral shoulder motion by about 40%, with significant reductions observed across all three tasks ($p < 0.01$), compared to the body-powered prosthesis. Muscle activation in the biceps, triceps, and deltoids was substantially lower with the myoelectric prosthesis, showing reductions ranging from 50% to 60% ($p < 0.001$). Additionally, pressure exerted on the users back by the harness was drastically reduced due to the lack of straps in the myoelectric application ($p < 0.001$) when using the myoelectric prosthesis.

INDEX TERMS Myoelectric prosthesis, body-powered prosthesis, performance sensing, electromyography control.

I. INTRODUCTION

In the United States, currently about 41,000 individuals are registered for upper limb loss, but only half of this population uses a prosthetic device [1]. Upper limb loss occurs over a broad age range due to accidents, disease, or congenital causes [2]. Various types of prosthetic devices are used by amputees to restore partial function of the missing arm in order to perform activities of daily living. However, approximately 38% of upper limb prosthesis users report dissatisfaction with their current devices due to limited functionality, discomfort, and impediments to sensory feedback [3]. Rejection rates as high as 35–45% have been reported [4], with contributing factors including

The associate editor coordinating the review of this manuscript and approving it for publication was Paolo Crippa.

© 2026 The Authors. This work is licensed under a Creative Commons Attribution 4.0 License.
For more information, see https://creativecommons.org/licenses/by/4.0/

excessive weight, limited functionality, insufficient training, device maintenance burden, repair cost, and reduced productivity [5].

Two widely used prosthetic solutions over the past several decades are body-powered and myoelectric prostheses. Body-powered prostheses incorporate a Bowden cable attached to a shoulder harness, such that movement of the shoulder or torso generates cable excursion to actuate the terminal device (e.g., a hook). In contrast, myoelectric prostheses use surface electromyography (sEMG) sensors to capture muscle activation signals and actuate the terminal device using an electric motor. Because these two systems rely on fundamentally different actuation strategies, they impose distinct biomechanical and cognitive demands on users.

As the most commonly prescribed upper-limb prosthetic options, body-powered and myoelectric devices have been extensively compared from qualitative, clinical, and usability perspectives. These comparisons often focus on cosmesis, comfort, and control strategy [6]. Myoelectric prostheses generally provide superior cosmesis and eliminate the need for shoulder harnesses, which can improve comfort during prolonged use [6]. Additionally, myoelectric control is often perceived as more psychologically natural due to the direct mapping between muscle activation and prosthetic motion [6]. Recent advances further demonstrate the broader potential of sEMG for gesture recognition [7], kinematic estimation [8], and neuromuscular assessment [9], [10]. However, myoelectric systems are also subject to challenges related to signal variability, control robustness, training requirements, and device cost [11]. Perspective-based analyses further emphasize that prosthesis preference and long-term acceptance depend strongly on individual user characteristics, training history, and task demands, rather than actuation type alone [12].

Body-powered prostheses, on the other hand, are valued for their mechanical simplicity, durability, and robustness to environmental contamination. They also provide extended proprioceptive feedback through cable tension, allowing users to modulate grip force via shoulder or trunk motion [13]. Nevertheless, multiple studies have shown that body-powered devices require greater activation of upper-limb and trunk musculature to actuate the terminal device, leading to increased compensatory movements and localized discomfort, particularly in the shoulders and back during long-term use [6], [11]. A number of quantitative studies have investigated biomechanical and functional differences between body-powered and myoelectric prostheses. Prior work has examined kinematics [11], [14], [15], grip control [16], force feedback [17], cable forces [18], and embodiment [19]. Carey et al. [15] presented a case study of a transradial amputee and reported increased shoulder and elbow motion during body-powered prosthesis use, reflecting compensatory strategies associated with cable-driven actuation. Finco et al. [14] similarly observed altered shoulder and elbow kinematics when comparing body-powered and myoelectric prostheses, though results varied across tasks and participants. Razak et al. [20] further demonstrated that different prosthetic actuation mechanisms significantly influence elbow joint biomechanics and loading patterns when compared to normal limb function.

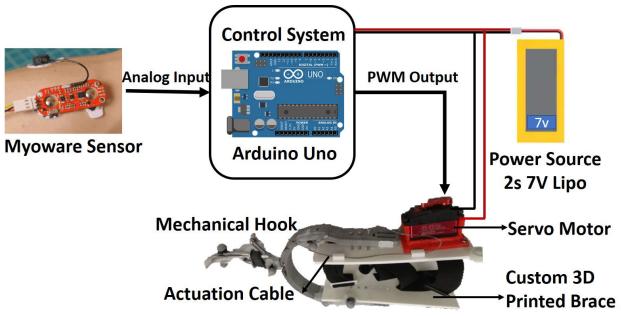


FIGURE 1. Schematic of Myoware system showing the electric diagram and the main components: sEMG sensor, control system, power source, servo motor, 3D-printed brace, and mechanical hook.

In addition to biomechanical outcomes, embodiment and user experience have been explored as critical factors in prosthesis evaluation. Engdahl et al. [19] reported that embodiment differences between body-powered and myoelectric prostheses were not solely determined by actuation strategy, but were also influenced by factors such as cause of limb absence and daily prosthesis wear time. A broader synthesis of these findings is provided by Engdahl et al. [12], who emphasize that the benefits and limitations of body-powered and myoelectric prostheses are highly context-dependent and cannot be fully captured by any single performance metric.

Despite these valuable contributions, controlled quantitative comparisons between body-powered and myoelectric prostheses remain methodologically challenging. Existing studies differ substantially in prosthetic interface design, residual limb characteristics, user experience level, and task conditions, making it difficult to isolate the physiological effects of actuation strategy alone. In particular, few studies have evaluated both control modes under identical mechanical interfaces while holding task conditions constant.

In the present study, we propose a modular retrofit solution that preserves the mechanical design of body-powered devices while enabling myoelectric actuation. This approach facilitates both controlled comparisons with an identical interface and suggests a cost-efficient technology transition from body-powered to myoelectric prosthesis. Ten non-amputee participants were recruited as a feasibility study group to validate the plug-and-play prosthesis module and explore differences in user response.

II. DEVICE DESCRIPTION

The modular system consists of the Myoware actuation system, a custom 3D-printed bypass brace, and the mechanical linkage required for integration with the body-powered

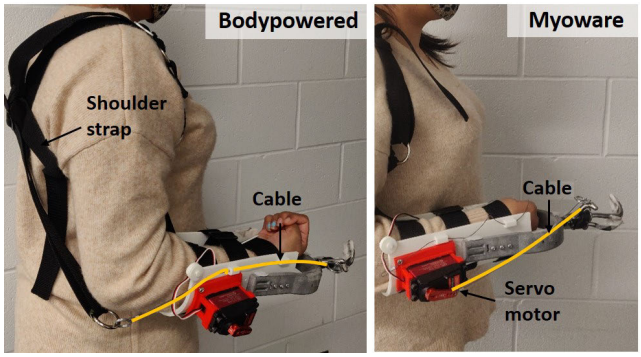


FIGURE 2. A participant wearing (a) body-powered prosthetic setup and (b) Myoware prosthetic setup for the experiment.

prosthesis. This design aims to support both research evaluation and potential clinical translation with minimal hardware modification or user retraining. The Myoware system primarily consists of five major components: sEMG sensors, a microcontroller, a power source, a servo motor, and a prosthetic hook built on a custom 3D-printed upper arm brace as shown in Fig. 1. The upper arm brace was mounted on the right side of the user to bypass the forearm of non-amputee participant for the experiment. A Hosmer hook F5X (Fillauer, TN) was mounted on a 3D-printed upper arm brace. The hook was part of an off-the-shelf body-powered prosthesis that uses a cable linked to a shoulder strap to open and close the hook (Fig. 2a). This hook is usually kept closed by a rubber band, but it can be voluntarily opened when the user causes cable excursion with shoulder and trunk movement to pull the lever of the hook.

For the Myoware prosthesis, a servo motor was used to open and close the hook as shown in Fig. 2b. An sEMG sensor was placed on the Brachioradialis to record the desired muscle activity needed to open or close the hook. The muscle activity was measured to control the opening and closing of the hook. The microcontroller Uno (Arduino, Italy) is a board with a microprocessor. It contains 14 digital I/O pins, 6 analog inputs, a 16 MHz ceramic resonator, a USB connection, a power connector, an ICSP header, and a reset button. It can be connected to a computer through USB or powered using an AC-to-DC converter or battery. It employs an Atmega328P configured as a USB-to-serial converter. The Arduino Uno received the sEMG input from the Myoware sensor (Advancer Technologies, NC) and mapped the input muscle signals to the angle of the servo motor using Pulse Width Modulated (PWM) signals. The Myoware sensor provided a rectified and enveloped sEMG signal for control. Myoware muscle sensor measures muscle activity of the muscle through the electrical potential of the muscle known as surface electromyography (sEMG). sEMG signals are generated by the electrical activity associated with muscle contraction and are detected by the sensor. Myoware muscle sensor is designed to be used directly with a microcontroller. The Myoware sensor output is an amplified, rectified and integrated EMG signal. The input voltage required for the Myoware muscle sensor is +3.3 V to +5 V, and its bandwidth is approximately 10–400 Hz. A servo motor LD-27MG (Hiwonder, China) was installed to open and close the tensioned prosthetic hook. The servo motor produces more than a minimum required torque of 22 kg-cm to actuate the tensioned hook. The servo motor was mounted on the forearm brace and connected to the hooks lever using a metal string to the servo arm for the actuation. The controller is described in Algorithm 1. The controller requires three threshold values. T_T, T_H, and T_L stand for muscle trigger threshold, high muscle activity threshold, and low muscle activity threshold. Because these threshold values differ between participants, they were determined before the experiment started and set as constant variables in the microcontroller based on individual participant's MVC and baseline noise floor.

The conversion from the body-powered to the myoelectric configuration is achieved through a detachable plug-and-play actuation module. In the body-powered mode, the prosthetic hook is actuated via a Bowden cable connected to a shoulder harness. To convert the system to a myoelectric configuration, the shoulder harness and cable are removed, and the electrical module is strapped onto the same forearm brace using adjustable fastening straps. The existing mechanical hook remains unchanged and is mechanically coupled to a servo motor within the electrical module via a direct linkage to the hook lever. In this configuration, the servo motor replaces the cable-driven actuation, enabling electrically driven opening and closing of the same hook without modifying the underlying mechanical interface or socket alignment.

Algorithm 1 Myoware-Servo Control Algorithm

Input: E_1 and E_2

while True **do**
  Read E_1 from EMG1
  Read E_2 from EMG2
  if $E_1 > t_T$ **then**
    activation
    if ($E_2 > t_H$ and $P > P_{open,half}$) **then**
      $P \leftarrow P - 100$
      if $P \leq P_{open,full}$ **then**
        $P \leftarrow P_{open,full}$
      end if
    end if
  end if
  if $E_2 < t_L$ **then**
    $P \leftarrow P + 100$
    if $P \geq P_{close}$ **then**
      $P \leftarrow P_{close}$
    end if
  end if
  if t_L<$E2$<t_H **then**
    $P \leftarrow P$
  end if
end while

Notation:

- E_1, E_2: sEMG signals from wrist muscles
- t_H: High activation threshold for E_2
- t_L: Low activation threshold for E_2
- t_T: Trigger threshold for E_1
- P: Pulse width (in microseconds) sent to servo
- $P_{open,full}$: PWM value to fully open the hook
- $P_{open,half}$: PWM value to half-open the hook
- P_{close}: PWM value to close the hook

III. HUMAN EXPERIMENT

A. PROTOCOL

Ten healthy adults (9 male and 1 female) signed a written consent form approved by the Institutional Review Board (IRB) of University at Buffalo before the experiment. Participants were recruited through word of mouth and flyers. The inclusion criteria specify that participants must be between 18 and 65 years of age and be healthy and physically capable of independently performing activities of daily living. Individuals will be excluded if they have any neurological conditions, a history of upper limb amputation with current prosthesis use, severe obstructive pulmonary disease or cardiac conditions that limit activity, upper extremity orthopedic conditions, sensory loss, seizure disorders, severe arthritis, or uncontrolled hypertension that restrict daily activities. The sample size was established based on established guidelines for feasibility studies [21], [22], [23]. The whole experimental data collection involves three different tasks with three forearm set-ups: freehand, body-powered prosthetic hook, and Myoware prosthetic hook. The order of the forearm set-ups is pseudo-randomly assigned to the participant. Each task was performed for eight consecutive cycles with two minutes of rest between each cycle. The eight cycles were used to obtain a representative and repeatable estimate of the participant's kinematic and physiological response while maintaining a practical total testing duration. This choice is consistent with upper-limb biomechanical benchmarking recommendations suggesting at least eight repetitions per motor skill as a compromise between data robustness, repeatability, and protocol duration [24], [25]. A two-minute seated rest period was provided between testing conditions to reduce the potential influence of muscular fatigue and carryover between prosthetic modes, consistent with rest intervals used in comparable myoelectric and prosthetic-hand testing protocols [26], [27] (Fig 3).

The user response on different arm set-ups was measured using three different sensor systems to track the subjects body movements and muscle activity: an optical motion capture system, sEMG sensors, and pressure sensors. Reflective markers were placed on the subjects body to track the body movements with ten motion capture cameras Vero v2.2 (Vicon, UK). The reflective markers were attached to the subject to compute the posture of head, torso, left shoulder, right shoulder, and right elbow as shown in Fig. 4. The markers were also attached on the upper arm brace and the prosthetic hook. Trigno wireless EMG system T03-A16014

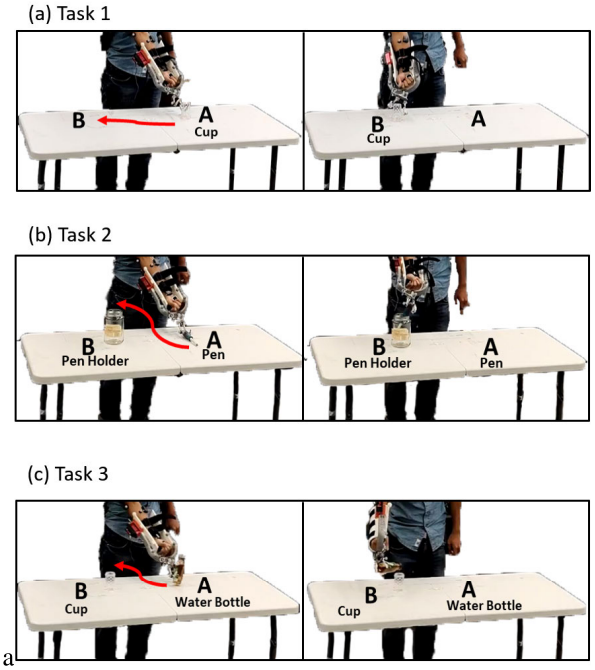


FIGURE 3. Subject performing the tasks wearing the Myoware prosthesis. (a) Pick and place of a cup (b) Pick and place a pen in a pen holder (c) Pour water into a cup.

(Delsys, MA) allowed us to monitor the activity of the different muscle groups to show the difference in muscle efforts during different testing cycles. The placements of the sEMG Sensors were as follows: right flexor carpi radialis, right extensor carpi radialis, right biceps brachii, right triceps brachii, left/right deltoid, as shown in Fig. 4. Pressure sensors SEN-09375 (SparkFun, CO) were placed below the harness straps, to measure the pressure that the harness is applying on the participants back.

Three representative activities of daily living (ADL) were performed to compare physiological changes when using different prosthetic devices: Task 1 moving a cup, Task 2 organizing a pen, and Task 3 pouring water into a cup. There were two marked points A and B on the table which were 30 cm apart. Prior to data collection, EMG thresholds were calibrated individually for each participant during a brief calibration session. Participants were instructed to perform repeated voluntary wrist flexion and relaxation cycles. Thresholds were set relative to each participants baseline noise and maximum voluntary contraction to ensure reliable activation without false triggering. The subject was asked to stand 30 cm away from the midpoint between points A and B.

Task 1 is to move a glass from the point A to the point B marked on a table as demonstrated in Fig. 3(a). Task 2 is picking up a pen on the table at point A and placing it into a pen holder on the point B. The cycle began when the subject placed the prosthetic hook directly over the point A and ended when the pen was put down in the holder. Task 3 is picking

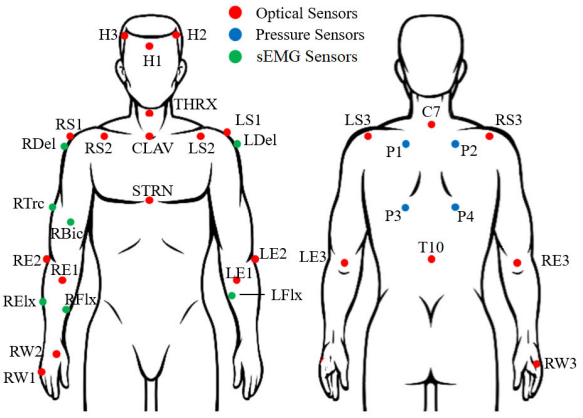


FIGURE 4. Positions of the reflective markers, pressure sensors, and sEMG sensors on the subject. Marker and sEMG placement followed established biomechanical and surface EMG guidelines [29], [30].

up a glass of water from point A and moving it over to the point B, pouring it into the glass at the point B, and then placing the glass back at point A. All participants were asked to keep their lower limbs stationary during the trials.

Time synchronization across the motion capture, sEMG, and pressure sensing systems was achieved using the Vicon Lock Sync hardware interface. The Vicon motion capture system served as the primary clock, while third-party devices including the Delsys Trigno sEMG system and pressure sensors were integrated through the Lock Sync (Vicon, UK) input/output module. Lock Lab and Lock Studio software were used to configure, control, and verify synchronized data acquisition across all systems. This hardware-based synchronization ensured consistent timestamp alignment and minimized temporal offsets between kinematic, muscle activation, and pressure measurements during all experimental trials.

B. DATA ANALYSIS

1) EULER ANGLES (SHOULDER AND ELBOW)

The Euler angles were calculated to show the changes in the orientation of the upper limb. A rotation matrix was calculated between the fixed frames and the normal vector to the planes formed by the three marker points on each body segment. The calculated rotation matrix was used to compute the Euler angles [28]. The xyz rotation representing Euler angles were used where the α is the rotation about x-axis (yaw), β is the rotation about y-axis (roll), and γ is the rotation about z-axis (pitch) as shown in Fig. 5. The three Euler angles (α, β, γ) represent the upper limb joint angles with respect to the T-pose while performing the tasks.

2) TRUNK MOVEMENTS

Trunk angles have been created to measure trunk coronal range of motion, trunk sagittal range of motion, and the back-shoulder protraction/retraction angle. Fig. 6 shows the definition of the trunk and back-shoulder angles. The sagittal trunk angle measures the forward and backward movement

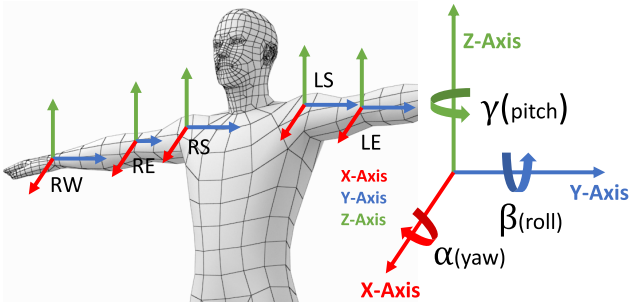


FIGURE 5. Construction of the coordinates for computing Euler angles. All angles are computed with respect to the T-pose. Adapted from Slabaugh, 1999 [28].

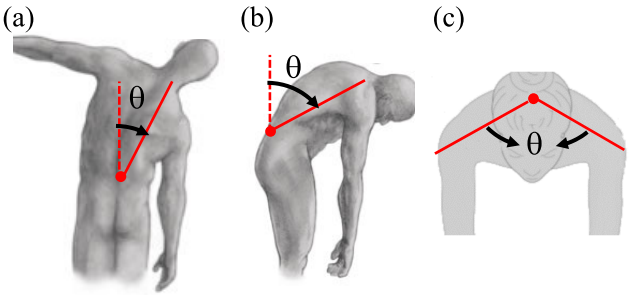


FIGURE 6. (a) Coronal range of motion of the trunk. (b) Sagittal range of motion of the trunk. (c) Protraction/retraction angle between the shoulders and the neck. Angle definitions are based on established marker-based kinematic approaches [31], [32].

of the trunk using the reflective markers at C7 and T10. The coronal trunk angle measures the sideways movement of the trunk using the markers at clavicle, C7, and T10. The back-shoulder (protraction/retraction) angle is measured by using right/left shoulders and C7 markers.

3) sEMG ANALYSIS

After the sEMG data were collected through the Delsys Trigno system, the data were processed using a fourth-order Butterworth band-pass filter ranging from 50 to 500 Hz to retain the dominant muscle activation spectrum while attenuating motion artifacts and high-frequency noise. The filtered signal was then full-wave rectified and smoothed using a low-pass Butterworth filter with a 6 Hz cutoff to extract the linear envelope of muscle activation. This preprocessing pipeline and selection of cutoff frequencies are consistent with established sEMG processing practices for myoelectric prosthetic control and human–prosthesis interaction studies [33], [34]. The sEMG data were normalized using each participants maximum and minimum sEMG values obtained during a standardized calibration procedure conducted prior to task execution. This normalization approach reduces inter-subject variability in EMG amplitude and is commonly employed in myoelectric prosthetic control studies to enable comparison across users [33], [34].

4) STATISTICAL ANALYSIS

For each participant, the outcome measures from the eight repetitions of each task and condition were averaged to obtain

one participant-level value. From the individual participant data, peak values of range of motion, sEMG, and pressure sensor measurements were compiled into group-level data for statistical analysis. For each outcome variable, a repeated-measures analysis of variance (rANOVA) was performed to compare the three forearm conditions—freehand, body-powered, and Myoware—across the three experimental tasks. Prior to each rANOVA, Mauchly's test was used to assess the assumption of sphericity, and Greenhouse–Geisser-corrected results were reported when this assumption was violated. When appropriate, post-hoc pairwise comparisons between conditions were conducted using paired t-tests with Holm–Bonferroni correction [35]. Effect sizes for pairwise comparisons were calculated using Pearson's r, derived from the corresponding t-statistic and degrees of freedom, to quantify the magnitude of the differences independent of sample size. Statistical significance was assessed at $p < 0.05$. All statistical analyses were performed using SPSS Statistics version 26.0 (IBM Corp., Armonk, NY, USA).

IV. RESULTS

The group-level results were compiled to compare different measurements such as kinematic range of motion, sEMG values, and maximum pressure sensor values. The repeated-measures ANOVA results are presented alongside the corresponding outcome measures, while the post-hoc pairwise comparisons are summarized in Table 2.

The kinematic analysis was conducted on the range of motion of the shoulder and elbow. The right shoulder angles for pitch, roll, and yaw are presented in Fig. 7(a) across three different tasks. The right shoulder angles showed slight changes across the three prosthetic conditions, but no significant overall effect of prosthetic condition was observed for right shoulder roll, pitch, or yaw across the three tasks.

Instead, participants chose to use right elbow flexion/extension to perform the pick-and-place tasks. Prosthetic condition significantly affected right elbow flexion/extension in Task 1 [$F(2, 18) = 6.347$, $p < 0.01$], Task 2 ($F(2, 18) = 61.082$, $p < 0.001$), and Task 3 ($F(2, 18) = 21.651$, $p < 0.001$).

For pairwise comparisons of right elbow flexion/extension, none of the three comparisons were significant for Task 1 after Holm–Bonferroni correction. For Task 2, significant differences were observed for freehand–body-powered ($p < 0.005$, $r = 0.845$), body-powered–Myoware ($p < 0.001$, $r = 0.959$), and freehand–Myoware ($p < 0.001$, $r = 0.962$). In Task 3, significant differences were observed for freehand–body-powered ($p < 0.01$, $r = 0.739$), body-powered–Myoware ($p < 0.001$, $r = 0.891$), and freehand–Myoware ($p < 0.005$, $r = 0.833$).

In addition, left shoulder flexion/extension (pitch) showed a significant effect of prosthetic condition in Task 1 [$F(2, 18) = 8.369$, $p < 0.005$], Task 2 [$F(2, 18) = 70.195$, $p < 0.001$], and Task 3 [$F(2, 18) = 29.488$, $p < 0.001$].

The pairwise comparisons indicate that the body-powered condition produced a dominantly high range of motion in the left shoulder pitch angle. In Task 1, body-powered use differed significantly from freehand ($p < 0.05$, $r = 0.717$) and Myoware ($p < 0.01$, $r = 0.810$). In Task 2, body-powered use differed from freehand ($p < 0.001$, $r = 0.934$) and Myoware ($p < 0.001$, $r = 0.954$), while freehand also differed from Myoware ($p < 0.001$, $r = 0.871$). In Task 3, significant differences were observed for freehand–body-powered ($p < 0.005$, $r = 0.855$), body-powered–Myoware ($p < 0.001$, $r = 0.906$), and freehand–Myoware ($p < 0.05$, $r = 0.684$). This indicates that left shoulder flexion/extension was used to actuate the body-powered prosthesis to accomplish all three tasks.

TABLE 1. Peak values of pressure sensors placed along the back.

Pressure Pad	Free(Free-body)	body(body-myo)	Myo(Free-myo)
P1	107.014***	964.198***	100.145
P2	100.44***	960.865***	105.98
P3	96.316***	927.261***	104.213
P4	94.301***	948.637***	104.21

*** indicates p<0.001 for the pairwise comparison.

The trunk range of motion in coronal and sagittal planes was also measured as shown in Fig. 7(b). In general, trunk movement shows the highest range of motion with body-powered device and the smallest movement with free hand. The trunk coronal angle, which indicates the sideways tilting of the torso, showed a significant effect of prosthetic condition in each task: $F(1.283, 11.55) = 59.787$, $p < 0.001$ for Task 1; $F(2, 18) = 99.542$, $p < 0.001$ for Task 2; and $F(1.27, 11.43) = 60.690$, $p < 0.001$ for Task 3.

For Task 1, the coronal-plane pairwise comparisons were significant for freehand–body-powered ($p < 0.001$, $r = 0.958$), body-powered–Myoware ($p < 0.001$, $r = 0.869$), and freehand–Myoware ($p < 0.001$, $r = 0.948$). For Task 2, significant differences were observed for freehand–body-powered ($p < 0.001$, $r = 0.965$), body-powered–Myoware ($p < 0.001$, $r = 0.962$), and freehand–Myoware ($p < 0.001$, $r = 0.919$). For Task 3, significant differences were observed for freehand–body-powered ($p < 0.001$, $r = 0.951$), body-powered–Myoware ($p < 0.001$, $r = 0.894$), and freehand–Myoware ($p < 0.001$, $r = 0.945$). These results show a significant deviation in coronal range of motion depending on the type of prosthesis.

The sagittal plane gives information about the trunk forward-backward movement. Similar to the coronal plane, significant effects were observed in Task 1 ($F(2, 18) = 153.153$, $p < 0.001$), Task 2 ($F(2, 18) = 31.425$, $p < 0.001$), and Task 3 ($F(1.29, 11.62) = 271.511$, $p < 0.001$).

For Task 1, significant sagittal-plane differences were observed for freehand–body-powered ($p < 0.001$, $r = 0.985$), body-powered–Myoware ($p < 0.001$, $r = 0.893$), and freehand–Myoware ($p < 0.001$, $r = 0.977$). For Task 2, significant differences were observed for freehand–body-powered ($p < 0.001$, $r = 0.902$), body-powered–Myoware ($p < 0.005$, $r = 0.843$), and freehand–Myoware ($p < 0.005$, $r = 0.847$). For Task 3, significant differences

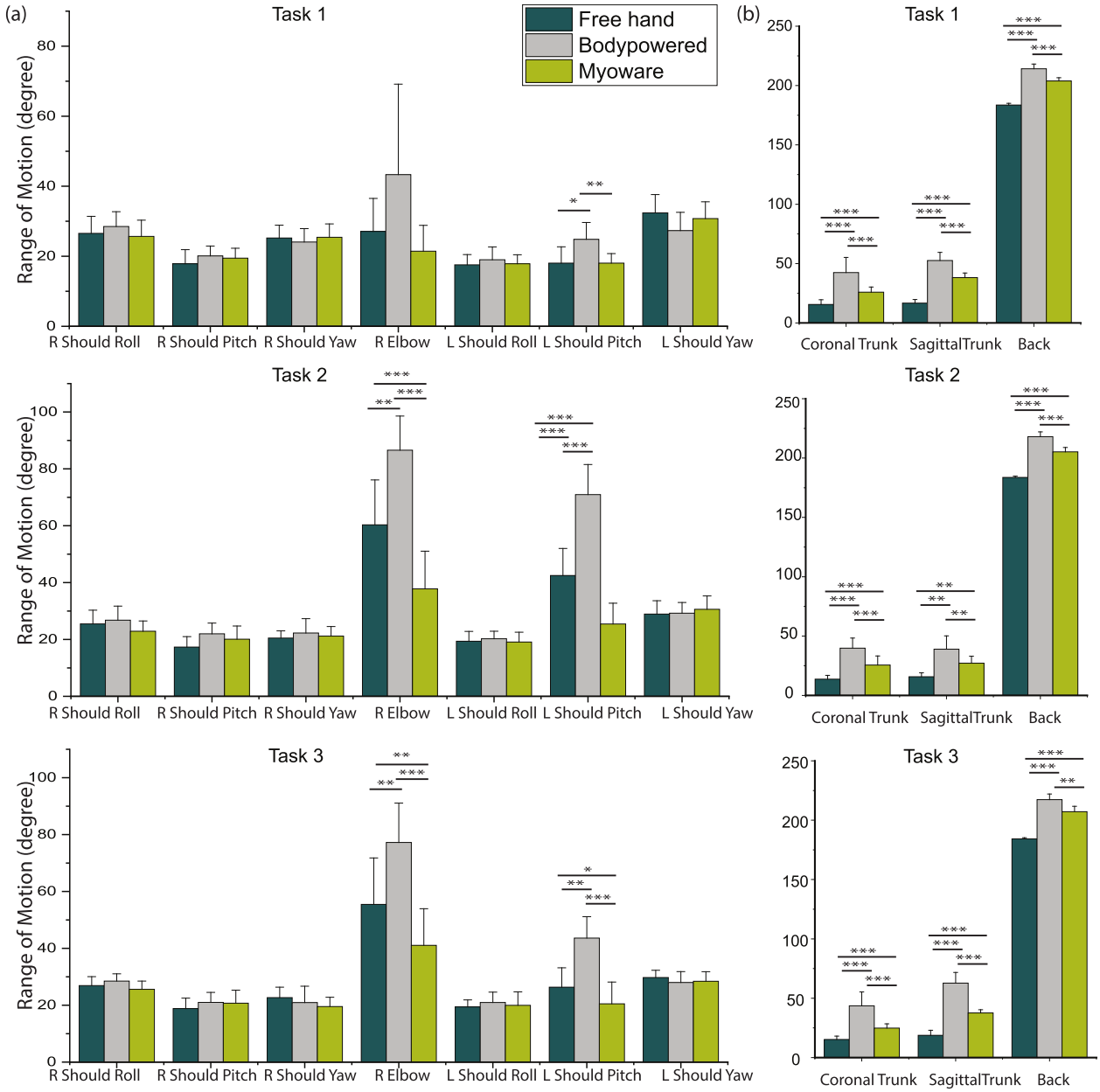


FIGURE 7. (a) Kinematics of the upper limb including right shoulder, right elbow, and left shoulder (b) Kinematics of the trunk including coronal, sagittal, and back for Tasks 1, 2, and 3. *P<0.05, **P<0.01, and ***P<0.001.

were observed for freehand–body-powered ($p < 0.001$, $r = 0.989$), body-powered–Myoware ($p < 0.001$, $r = 0.967$), and freehand–Myoware ($p < 0.001$, $r = 0.988$).

In accordance with the above two factors, the back angle, which is the shoulder protraction/retraction angle, shows a similar pattern in Task 1 ($F(2, 18) = 266.982$, $p < 0.001$), Task 2 ($F(1.22, 10.97) = 288.665$, $p < 0.001$), and Task 3 ($F(1.26, 11.38) = 185.614$, $p < 0.001$).

For Task 1, significant back-angle differences were observed for freehand–body-powered ($p < 0.001$, $r = 0.988$), body-powered–Myoware ($p < 0.001$, $r = 0.911$), and freehand–Myoware ($p < 0.001$, $r = 0.994$). For Task 2, significant differences were observed for freehand–body-powered ($p < 0.001$, $r = 0.995$), body-powered–Myoware ($p < 0.001$, $r = 0.910$), and freehand–Myoware ($p < 0.001$, $r = 0.989$). For Task 3, significant differences were observed for freehand–body-powered ($p < 0.001$, $r = 0.993$), body-powered–Myoware ($p < 0.005$, $r = 0.823$), and freehand–Myoware ($p < 0.001$, $r = 0.983$).

This analysis indicates that the trunk movement in body-powered prosthesis consists of two different components. The significant distinction between the Myoware prosthesis and the free hand shows that the prosthetic use generates compensatory motion of the trunk. Furthermore,

TABLE 2. Post-hoc pairwise comparisons across all metrics. Values are reported as Bonferroni-Holm adjusted p-value (effect size *r*).

	Task 1			Task 2			Task 3		
Metric	F–B	B–M	F–M	F–B	B–M	F–M	F–B	B–M	F–M
Range of Motion									
RSR	0.812 (0.284)	0.812 (0.364)	0.812 (0.140)	0.576 (0.190)	0.220 (0.553)	0.220 (0.560)	0.749 (0.297)	0.045 (0.708)	0.749 (0.261)
RSP	0.456 (0.462)	0.813 (0.187)	0.813 (0.279)	0.014 (0.780)	0.438 (0.275)	0.438 (0.403)	0.820 (0.362)	0.840 (0.076)	0.840 (0.271)
RSY	1.000 (0.200)	1.000 (0.271)	1.000 (0.036)	1.000 (0.270)	1.000 (0.201)	1.000 (0.181)	0.725 (0.305)	0.725 (0.205)	0.214 (0.563)
REL	0.088 (0.627)	0.088 (0.653)	0.088 (0.633)	0.001 (0.845)	< 0.001 (0.959)	< 0.001 (0.962)	0.009 (0.739)	< 0.001 (0.891)	0.003 (0.833)
LSR	1.000 (0.298)	1.000 (0.319)	1.000 (0.073)	1.000 (0.191)	1.000 (0.251)	1.000 (0.062)	0.486 (0.453)	0.980 (0.233)	0.980 (0.104)
LSP	0.026 (0.717)	0.008 (0.810)	0.999 (0.000)	< 0.001 (0.934)	< 0.001 (0.954)	< 0.001 (0.871)	0.002 (0.855)	< 0.001 (0.906)	0.020 (0.684)
LSY	0.160 (0.596)	0.207 (0.517)	0.428 (0.266)	1.000 (0.090)	1.000 (0.216)	1.000 (0.227)	0.771 (0.374)	0.771 (0.138)	0.771 (0.324)
Trunk Kinematics									
C	< 0.001 (0.958)	< 0.001 (0.869)	< 0.001 (0.948)	< 0.001 (0.965)	< 0.001 (0.962)	< 0.001 (0.919)	< 0.001 (0.951)	< 0.001 (0.894)	< 0.001 (0.945)
S	< 0.001 (0.985)	< 0.001 (0.893)	< 0.001 (0.977)	< 0.001 (0.902)	0.002 (0.843)	0.002 (0.847)	< 0.001 (0.989)	< 0.001 (0.967)	< 0.001 (0.988)
B	< 0.001 (0.988)	< 0.001 (0.911)	< 0.001 (0.994)	< 0.001 (0.995)	< 0.001 (0.910)	< 0.001 (0.989)	< 0.001 (0.993)	0.002 (0.823)	< 0.001 (0.983)
Electromyography									
RF	0.002 (0.831)	< 0.001 (0.994)	< 0.001 (0.973)	0.004 (0.792)	< 0.001 (0.986)	< 0.001 (0.992)	< 0.001 (0.936)	< 0.001 (0.992)	< 0.001 (0.994)
RE	0.243 (0.385)	0.002 (0.857)	0.060 (0.652)	0.485 (0.385)	0.021 (0.756)	0.485 (0.307)	0.674 (0.143)	0.506 (0.402)	0.506 (0.447)
RB	< 0.001 (0.981)	< 0.001 (0.998)	0.010 (0.732)	< 0.001 (0.989)	< 0.001 (0.997)	0.040 (0.624)	< 0.001 (0.991)	< 0.001 (0.997)	0.845 (0.067)
RT	< 0.001 (0.975)	< 0.001 (0.991)	0.047 (0.608)	< 0.001 (0.983)	< 0.001 (0.998)	0.253 (0.377)	< 0.001 (0.977)	< 0.001 (0.995)	0.312 (0.336)
RD	< 0.001 (0.973)	< 0.001 (0.990)	0.159 (0.456)	< 0.001 (0.986)	< 0.001 (0.997)	0.164 (0.451)	< 0.001 (0.985)	< 0.001 (0.995)	0.017 (0.699)
LD	< 0.001 (0.975)	< 0.001 (0.979)	0.301 (0.344)	< 0.001 (0.989)	< 0.001 (0.995)	0.725 (0.120)	< 0.001 (0.989)	< 0.001 (0.996)	0.015 (0.708)

F–B: Freehand versus Body-powered; B–M: Body-powered versus Myoelectric; F–M: Freehand versus Myoelectric prosthesis comparisons.

actuation of the body-powered hook causes additional trunk movement, which is manifested by a significant difference between the body-powered and Myoware conditions.

The sEMG analysis demonstrates the extra muscle activity and usage when performing the tasks with body-powered prosthesis compared to the Myoware prosthesis as shown in Fig. 8. The right flexor carpi radialis showed a significant effect of prosthetic condition in Task 1 ($F(1.27, 11.43) = 237.493$, $p < 0.001$), Task 2 ($F(2, 18) = 320.301$, $p < 0.001$), and Task 3 ($F(2, 18) = 499.443$, $p < 0.001$).

For Task 1, significant right-flexor differences were observed for freehand–body-powered ($p < 0.005$, $r = 0.831$), body-powered–Myoware ($p < 0.001$, $r = 0.994$), and freehand–Myoware ($p < 0.001$, $r = 0.973$). For Task 2, significant differences were observed for freehand–body-powered ($p < 0.005$, $r = 0.792$), body-powered–Myoware ($p < 0.001$, $r = 0.986$), and freehand–Myoware ($p < 0.001$, $r = 0.992$). For Task 3, significant differences were observed for freehand–body-powered ($p < 0.001$, $r = 0.936$), body-powered–Myoware ($p < 0.001$, $r = 0.992$), and freehand–Myoware ($p < 0.001$, $r = 0.994$). The right flexor showed the highest activation during Myoware use because the Myoware uses the flexor as the trigger to open and close the hook. On the other hand, significantly lower flexor muscle activation is observed when using the body-powered device.

For the right extensor carpi radialis, only Task 1 showed a significant overall change ($F(2, 18) = 8.866$, $p < 0.005$). For Task 1, body-powered use produced significantly greater extensor activation than Myoware ($p < 0.005$, $r = 0.857$), whereas the freehand–body-powered and freehand–Myoware comparisons were not significant. The omnibus effects were not significant for Task 2 ($F(2, 18) = 3.120$) or Task 3 ($F(2, 18) = 1.346$).

Both biceps brachii and triceps brachii showed significant overall differences across the three conditions. For the biceps brachii, the results were $F(1.28, 11.58) = 306.728$, $p < 0.001$ for Task 1; $F(1.17, 10.55) = 552.124$, $p < 0.001$ for Task 2; and $F(2, 18) = 500.961$, $p < 0.001$ for Task 3. For the triceps brachii, the results were $F(1.296, 11.66) = 223.674$, $p < 0.001$; $F(1.09, 9.85) = 337.499$, $p < 0.001$; and $F(1.13, 10.12) = 249.741$, $p < 0.001$ for Tasks 1–3, respectively.

In the biceps and triceps muscles, the body-powered condition showed significantly greater activation than both freehand and Myoware. For the biceps in Task 1, body-powered activation was greater than freehand ($p < 0.001$, $r = 0.981$) and Myoware ($p < 0.001$, $r = 0.998$). In Task 2, body-powered activation was greater than freehand ($p < 0.001$, $r = 0.989$) and Myoware ($p < 0.001$, $r = 0.997$). In Task 3, body-powered activation was greater than freehand ($p < 0.001$, $r = 0.991$) and Myoware ($p < 0.001$, $r = 0.997$). For the triceps in Task 1, body-powered activation was greater than freehand ($p < 0.001$, $r = 0.975$) and Myoware ($p < 0.001$, $r = 0.991$). In Task 2, body-powered activation was greater than freehand ($p < 0.001$, $r = 0.983$) and Myoware ($p < 0.001$, $r = 0.998$). In Task 3, body-powered activation was greater than freehand ($p < 0.001$, $r = 0.977$) and Myoware ($p < 0.001$, $r = 0.995$). These observations in the biceps brachii and triceps brachii correspond to the observations found in the elbow flexion/extension to perform the task.

The data from the left deltoid and right deltoid show a similar pattern to the biceps and triceps muscles. For the right deltoid, the overall results were $F(1.25, 11.2) = 184.483$, $p < 0.001$; $F(1.27, 11.45) = 323.111$, $p < 0.001$; and $F(1.23, 11.02) = 329.958$, $p < 0.001$. For the left deltoid, the corresponding results were $F(2, 18) = 154.070$, $p < 0.001$; $F(2, 18) = 395.257$, $p < 0.001$; and $F(2, 18) = 333.600$, $p < 0.001$ for Tasks 1–3, respectively.

Significant pairs in the left and right deltoids were driven primarily by the body-powered prosthesis. For the right

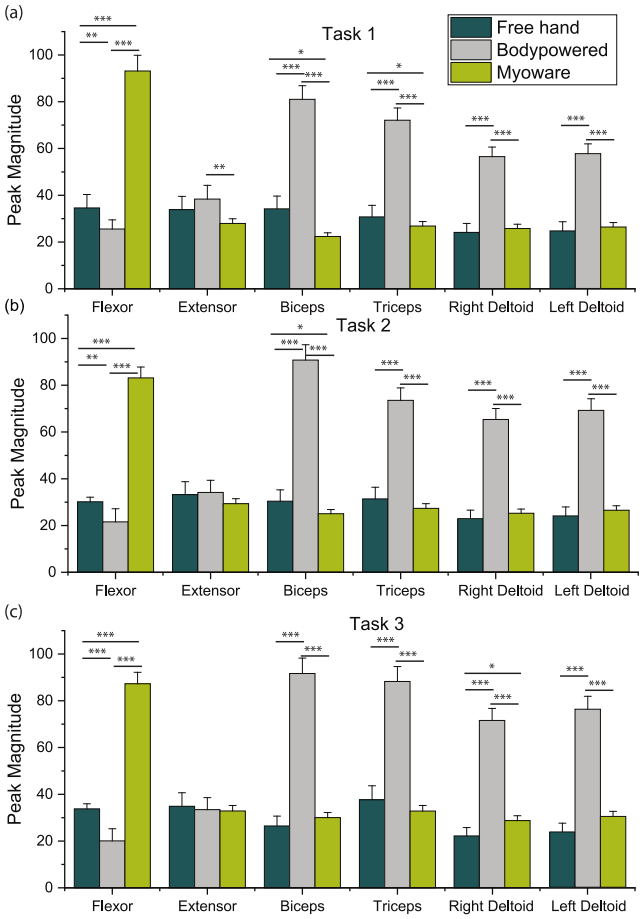


FIGURE 8. sEMG data from right flexor, right extensor, right biceps, right triceps, right deltoid, and left deltoid for (a) Task 1, (b) Task 2, and (c) Task 3.

deltoid in Task 1, body-powered activation was greater than freehand ($p < 0.001$, $r = 0.973$) and Myoware ($p < 0.001$, $r = 0.990$). In Task 2, body-powered activation was greater than freehand ($p < 0.001$, $r = 0.986$) and Myoware ($p < 0.001$, $r = 0.997$). In Task 3, body-powered activation was greater than freehand ($p < 0.001$, $r = 0.985$) and Myoware ($p < 0.001$, $r = 0.995$), while freehand also differed from Myoware ($p < 0.05$, $r = 0.699$). For the left deltoid in Task 1, body-powered activation was greater than freehand ($p < 0.001$, $r = 0.975$) and Myoware ($p < 0.001$, $r = 0.979$). In Task 2, body-powered activation was greater than freehand ($p < 0.001$, $r = 0.989$) and Myoware ($p < 0.001$, $r = 0.995$). In Task 3, body-powered activation was greater than freehand ($p < 0.001$, $r = 0.989$) and Myoware ($p < 0.001$, $r = 0.996$), while freehand also differed from Myoware ($p < 0.05$, $r = 0.708$). High left deltoid activation is expected from the high range of motion of the left shoulder; however, right deltoid also shows high activation. This is because, in order to keep the hook open, both deltoids had to be highly activated to maintain the shoulder posture against the force of the rubber band.

The results from the four pressure sensors in Table 1 show the overall p values being under ($p < 0.001$) for all three tasks. The comparative results show no significant difference between freehand and Myoware. However, comparisons involving the body-powered device show significant changes for all cases. The pressure sensors showed that higher pressure was exerted on the users back by the shoulder harness when using the body-powered prosthesis compared with the Myoware prosthesis.

V. DISCUSSION

A. KEY FINDINGS

This study compares the physiological responses associated with a conventional body-powered prosthesis and a plug-and-play Myoware prosthesis. Data were collected from ten subjects using both methods to perform a set of tasks. From all the above mentioned results, our hypothesis has been verified using different measures including joint angles, trunk angles, sEMG, and pressure values. Participants using the Myoware prosthesis showed less compensatory movement of shoulder, elbow, and trunk compared to the body-powered prosthesis. However, participants using the Myoware prosthesis showed increased range of motion of the trunk compared to performing the task with their own hand. This is because the Myoware prosthesis has significantly fewer degrees of freedom than the human forearm. Use of the Myoware prosthesis resulted in lower muscle activation compared to the body-powered prosthesis in the biceps, triceps, left deltoid, and right deltoid. Also, the data from the pressure sensors can be inferred to support that there is no additional stress on the back when using the Myoware prosthesis.

Beyond differences in peak pressure magnitude, the spatial distribution of pressure across the back reflects distinct load transfer mechanisms associated with each prosthetic configuration. In the body-powered condition, elevated pressure values were consistently observed across all pressure sensor locations, indicating sustained load transmission through the shoulder harness during task execution. This pressure pattern corresponds with the increased trunk flexion, lateral bending, and shoulder protraction observed in the kinematic analysis, suggesting that harness-induced forces contribute directly to compensatory upper-body motion. In contrast, the myoelectric configuration exhibited pressure profiles comparable to the freehand condition, consistent with the absence of a shoulder harness and reduced reliance on trunk-driven actuation. The reduced pressure distribution aligns with the observed decreases in trunk range of motion and shoulder compensation, indicating a coupled relationship between back loading and compensatory kinematic strategies.

From the range of motion data for the left shoulder, it can be shown that for all three tasks, body-powered prosthesis generates a higher range of motion for pitch angles because it uses the contralateral shoulder flexion and trunk rotation as the primary source of compensatory motion to operate the hook. Also, a general trend of higher deviation is shown in Tasks 2 and 3 compared to Task 1 because of the increased

complexity of the tasks. The right elbow also showed a significant increase in the body-powered case, because it requires outstretching of the elbow to generate tension in the string to keep the hook open to perform the tasks.

Looking at the group data for sEMG changes across the three tasks, in the case of the right flexor, the Myoware prosthesis has the highest value because it triggers to open the hook. The freehand case follows next as the participant flexed the wrist for grasping and moving the objects across all three tasks. body-powered has relatively low muscle activity because it only requires the extension of the arm to operate the hook. For the triceps and biceps, the body-powered condition required the highest muscle activity to maintain the hook open. This is presumably because the coactivation of the agonist and antagonist muscles increases the joint stiffness for locking the elbow motion when maintaining the opening of the hook. For the left and right deltoids, body-powered prosthesis generates the highest activity which increases from Task 1 to Task 3 due to the increased time to keep the hook open.

Compared to the results from previous studies which identified different kinematic characteristics of body-powered and Myoware prostheses, a greater range of elbow motion was observed in the case of body-powered prosthesis along with increased shoulder flexion and bending of the cervical spine as compensatory motion when performing the same task with different types of prostheses [15]. A similar conclusion has also been reached in the previous studies where amputees using a myoelectric device would exhibit less ROM for a given task compared to that of body-powered device [14], [36]. This is in accordance with the results obtained in our present study as shown in Fig. 7. While this study was conducted on non-amputee participants, certain kinematic and muscle activation trends observed, such as compensatory motion patterns and control strategies, are expected to carry over to amputee users due to the underlying mechanism of motion generation and interface design of the suggested plug-and-play module.

A consideration of the present study is the use of a non-amputee forearm bypass model to examine differences between body-powered and myoelectric prosthetic control. While non-amputee participants retain intact proprioception and neuromuscular coordination, which may influence movement strategies and sEMG activation patterns, this model allows systematic evaluation of prosthetic actuation effects under controlled conditions. Accordingly, the findings of this study offer insight into actuation-related trends in compensatory motion, muscle activation, and back loading, while motivating future investigations to extend these observations to amputee populations and real-world clinical contexts.

B. LIMITATIONS AND FUTURE WORK

The study has a few limitations in the study design. The experiment included only controlled pick-and-place tasks to move objects on the table. In the future, a greater variety of tasks spanning a broader task space could be included to test the performance of the prosthetic devices. These tasks will require more delicate and complex manipulation, such as cutting food, applying a deodorant, etc. Unlike simple pick-and-place activities, these tasks involve fine motor control, multi-joint coordination, and interaction with compliant or curved surfaces, which more closely mirror daily life challenges faced by prosthesis users. Incorporating such functionally diverse and context-rich tasks in future studies will allow for a more comprehensive evaluation of prosthetic usability, user adaptation, and compensatory strategies under realistic conditions. The present study was conducted on non-amputee participants, which does not capture the unique characteristics of amputee users. Also, participants were bypassing their own forearm with a distal-offset configuration, which resulted in the increased length of the arm. This could be addressed by changing the bypass configuration from the distal offset to the dorsal offset in future studies [37].

The participants were assumed to be novice prosthesis users, and the experiment did not monitor long-term learning effects, which can change the performance over time. In addition, the current Myoware set-up requires manual tuning to identify the threshold, which can be replaced by an automatic tuning algorithm for different subjects. Also, adding sensory feedback could improve the user experience of controlling the prosthesis. Future work will expand this study to include amputee participants to verify clinical applicability, assess user satisfaction and control, and conduct long-term use studies to capture learning and adaptation effects.

Future versions of this work could also explore enhancements in socket design, which have shown promising results in improving both comfort and functionality for users of myoelectric prostheses [38]. Previous studies have found that up to 57 percent of users experience discomfort or pain from poor socket fit and long-term use [39]. In addition, meaningful sensory input has been reported to play a major role in whether users continue to wear their prosthesis over time [40]. These insights highlight the importance of addressing these clinical factors in future studies, especially with amputee participants.

VI. CONCLUSION

In this study, body-powered and myoelectric prosthetic control were compared using a plug-and-play modular system with a common mechanical interface. By changing only the actuation method, the study evaluates the physiological demands of each prosthesis type during representative activities of daily living. The myoelectric configuration significantly reduced compensatory upper-limb and trunk movements, shoulder and arm muscle activation, and back pressure compared to the body-powered prosthesis. These findings suggest that eliminating the shoulder harness and cable-driven actuation can reduce physical burden during task execution. Kinematic, sEMG, and pressure measurements

showed that differences between the two actuation methods were reflected across multiple physiological responses. Greater elbow and contralateral shoulder movements with the body-powered prosthesis were accompanied by increased proximal muscle activation and harness loading. In contrast, the myoelectric configuration reduced these compensatory demands. The plug-and-play platform therefore provides a controlled approach for investigating how prosthetic actuation methods influence user movement and physical effort. These findings should be interpreted within the scope of this feasibility study, which involved non-amputee novice users, controlled experimental tasks, objective outcome measures, and manually calibrated myoelectric thresholds. Accordingly, future work will extend the evaluation to amputee users and more functionally diverse tasks, incorporate subjective measures of comfort, fatigue, and usability, and implement automated or adaptive threshold calibration methods. Long-term evaluations will further examine user learning and adaptation during extended prosthesis use.

REFERENCES

[1] K. Ziegler-Graham, E. J. MacKenzie, P. L. Ephraim, T. G. Travison, and R. Brookmeyer, "Estimating the prevalence of limb loss in the United States: 2005 to 2050," *Arch. Phys. Med. Rehabil.*, vol. 89, no. 3, pp. 422–429, Mar. 2008.

[2] H. Akhondi and P. Maduri, *Upper Limb Amputation*. Treasure Island, FL, USA: StatPearl, 2020.

[3] S. M. Engdahl, B. P. Christie, B. Kelly, A. Davis, C. A. Chestek, and D. H. Gates, "Surveying the interest of individuals with upper limb loss in novel prosthetic control techniques," *J. NeuroEngineering Rehabil.*, vol. 12, no. 1, p. 53, Dec. 2015.

[4] E. A. Biddiss and T. T. Chau, "Upper limb prosthesis use and abandonment: A survey of the last 25 years," *Prosthetics Orthotics Int.*, vol. 31, no. 3, pp. 236–257, 2007.

[5] K. Østlie, I. M. Lesjø, R. J. Franklin, B. Garfelt, O. H. Skjeldal, and P. Magnus, "Prosthesis rejection in acquired major upper-limb amputees: A population-based survey," *Disab. Rehabil., Assistive Technol.*, vol. 7, no. 4, pp. 294–303, Jul. 2012.

[6] J. Uellendahl, "Myoelectric versus body-powered upper-limb prostheses: A clinical perspective," *J. Prosthetics Orthotics*, vol. 29, no. 4S, pp. P25–P29, 2017.

[7] Y. Wang, Y. Tian, J. Zhu, H. She, Y. Jiang, Z. Jiang, and H. Yokoi, "A hand gesture recognition strategy based on virtual-dimension increase of EMG," *Cyborg Bionic Syst.*, vol. 5, p. 0066, Jan. 2024.

[8] H. Zhang, B. Peng, L. Tian, O. W. Samuel, and G. Li, "Continuous Kalman estimation method for finger kinematics tracking from surface electromyography," *Cyborg Bionic Syst.*, vol. 5, Jan. 2024, Art. no. 0094.

[9] J. Ou, N. Li, H. He, J. He, L. Zhang, and N. Jiang, "Detecting muscle fatigue among community-dwelling senior adults with shape features of the probability density function of sEMG," *J. NeuroEngineering Rehabil.*, vol. 21, no. 1, Nov. 2024, Art. no. 196.

[10] N. Li, J. Ou, H. He, J. He, L. Zhang, Z. Peng, J. Zhong, and N. Jiang, "Exploration of a machine learning approach for diagnosing sarcopenia among Chinese community-dwelling older adults using sEMG-based data," *J. NeuroEngineering Rehabil.*, vol. 21, no. 1, p. 69, May 2024.

[11] S. L. Carey, D. J. Lura, and M. J. Highsmith, "Differences in myoelectric and body-powered upper-limb prostheses: Systematic literature review," *J. Rehabil. Res. Dev.*, vol. 52, no. 3, pp. 247–262, 2015.

[12] S. M. Engdahl, M. A. Gonzalez, C. Lee, and D. H. Gates, "Perspectives on the comparative benefits of body-powered and myoelectric upper limb prostheses," *J. NeuroEngineering Rehabil.*, vol. 21, no. 1, pp. 1–15, Aug. 2024.

[13] J. Kang, M. A. Gonzalez, R. B. Gillespie, and D. H. Gates, "A haptic object to quantify the effect of feedback modality on prosthetic grasping," *IEEE Robot. Autom. Lett.*, vol. 4, no. 2, pp. 1101–1108, Apr. 2019.

[14] G. Finco, K. Keener, W. Amonette, and T. Krouskop, "Kinematic comparison of body-powered and myoelectric prostheses in users with transradial amputations," in *Proc. Myoelectric Controls Symp.*, 2017, pp. 15–18.

[15] S. L. Carey, R. V. Dubey, G. S. Bauer, and M. J. Highsmith, "Kinematic comparison of myoelectric and body powered prostheses while performing common activities," *Prosthetics Orthotics Int.*, vol. 33, no. 2, pp. 179–186, 2009.

[16] M. Atzori and H. Müller, "Control capabilities of myoelectric robotic prostheses by hand amputees: A scientific research and market overview," *Frontiers Syst. Neurosci.*, vol. 9, p. 162, Nov. 2015.

[17] J. D. Brown, T. S. Kunz, D. Gardner, M. K. Shelley, A. J. Davis, and R. B. Gillespie, "An empirical evaluation of force feedback in body-powered prostheses," *IEEE Trans. Neural Syst. Rehabil. Eng.*, vol. 25, no. 3, pp. 215–226, Mar. 2017.

[18] M. Hichert, D. A. Abbink, A. N. Vardy, C. K. van der Sluis, W. G. M. Janssen, M. A. H. Brouwers, and D. H. Plettenburg, "Perception and control of low cable operation forces in voluntary closing body-powered upper-limb prostheses," *PLoS ONE*, vol. 14, no. 11, Nov. 2019, Art. no. e0225263.

[19] S. M. Engdahl, S. K. Meehan, and D. H. Gates, "Differential experiences of embodiment between body-powered and myoelectric prosthesis users," *Sci. Rep.*, vol. 10, no. 1, pp. 1–10, Sep. 2020.

[20] N. A. A. Razak, N. A. A. Osman, H. Gholizadeh, and S. Ali, "Biomechanics principle of elbow joint for transhumeral prostheses: Comparison of normal hand, body-powered, myoelectric and air splint prostheses," *Biomed. Eng. OnLine*, vol. 13, no. 1, pp. 1–14, 2014.

[21] S. A. Julious, "Sample size of 12 per group rule of thumb for a pilot study," *Pharmaceutical Statist.*, vol. 4, no. 4, pp. 287–291, Oct. 2005.

[22] M. A. Hertzog, "Considerations in determining sample size for pilot studies," *Res. Nursing Health*, vol. 31, no. 2, pp. 180–191, Apr. 2008.

[23] A. L. Whitehead, S. A. Julious, C. L. Cooper, and M. J. Campbell, "Estimating the sample size for a pilot randomised trial to minimise the overall trial sample size for the external pilot and main trial for a continuous outcome variable," *Stat. Methods Med. Res.*, vol. 25, no. 3, pp. 1057–1073, Jun. 2016.

[24] V. Longatelli, D. Torricelli, J. Tornero, A. Pedrocchi, F. Molteni, J. L. Pons, and M. Gandolla, "A unified scheme for the benchmarking of upper limb functions in neurological disorders," *J. NeuroEngineering Rehabil.*, vol. 19, no. 1, p. 102, Sep. 2022.

[25] V. Longatelli, C. B. Sanz-Morère, D. Torricelli, P. M. Hernández, E. Guanziroli, J. Tornero, F. Molteni, J. L. Pons, A. Pedrocchi, and M. Gandolla, "Experimental validation of an upper limb benchmarking framework in healthy and post-stroke individuals: A pilot study," *IEEE Trans. Neural Syst. Rehabil. Eng.*, vol. 32, pp. 2356–2365, 2024.

[26] F. Barontini, M. Van Straaten, M. G. Catalano, A. Thoreson, C. Lopez, R. Lennon, M. Bianchi, K. Andrews, M. Santello, A. Bicchi, and K. Zhao, "Evaluating the effect of non-invasive force feedback on prosthetic grasp force modulation in participants with and without limb loss," *PLoS ONE*, vol. 18, no. 5, May 2023, Art. no. e0285081.

[27] C. Piazza, A. M. Simon, K. L. Turner, L. A. Miller, M. G. Catalano, A. Bicchi, and L. J. Hargrove, "Exploring augmented grasping capabilities in a multi-synergistic soft bionic hand," *J. NeuroEngineering Rehabil.*, vol. 17, no. 1, p. 116, Dec. 2020.

[28] G. G. Slabaugh, "Computing Euler angles from a rotation matrix," *Retrieved August*, vol. 6, no. 2000, pp. 39–63, 1999.

[29] G. Wu, F. C. T. van der Helm, H. E. J. D. Veeger, M. Makhsous, P. Van Roy, C. Anglin, J. Nagels, A. R. Karduna, K. McQuade, X. Wang, F. W. Werner, and B. Buchholz, "ISB recommendation on definitions of joint coordinate systems of various joints for the reporting of human joint motion—Part II: Shoulder, elbow, wrist and hand," *J. Biomechanics*, vol. 38, no. 5, pp. 981–992, May 2005.

[30] H. J. Hermens, B. Freriks, C. Disselhorst-Klug, and G. Rau, "Development of recommendations for SEMG sensors and sensor placement procedures," *J. Electromyogr. Kinesiol.*, vol. 10, no. 5, pp. 361–374, Oct. 2000.

[31] A. W. Titus, S. Hillier, Q. A. Louw, and G. Inglis-Jassiem, "An analysis of trunk kinematics and gait parameters in people with stroke," *Afr. J. Disab.*, vol. 7, pp. 1–6, Mar. 2018.

[32] O. Rettig, B. Krautwurst, M. W. Maier, and S. I. Wolf, "Definition of anatomical zero positions for assessing shoulder pose with 3D motion capture during bilateral abduction of the arms," *BMC Musculoskeletal Disorders*, vol. 16, no. 1, Dec. 2015, Art. no. 383.

[33] K. Kim and J. Kang, "Subject-independent sEMG-based prosthetic control using MAMBA2 with domain adaptation," in *Proc. IEEE/RSJ Int. Conf. Intell. Robots Syst. (IROS)*, Oct. 2025, pp. 16673–16679.
[34] M. A. Gonzalez, C. Lee, J. Kang, R. B. Gillespie, and D. H. Gates, "Getting a grip on the impact of incidental feedback from body-powered and myoelectric prostheses," *IEEE Trans. Neural Syst. Rehabil. Eng.*, vol. 29, pp. 1–11, 2021.
[35] John H. McDonald, *Handbook of Biological Statistics*. Oxford, U.K.: Clarendon, 2014.
[36] J. A. Doeringer and N. Hogan, "Performance of above elbow body-powered prostheses in visually guided unconstrained motion tasks," *IEEE Trans. Biomed. Eng.*, vol. 42, no. 6, pp. 621–631, Jun. 1995.
[37] A. W. Wilson, D. H. Blustein, and J. W. Sensinger, "A third arm—Design of a bypass prosthesis enabling incorporation," in *Proc. Int. Conf. Rehabil. Robot. (ICORR)*, Jul. 2017, pp. 1381–1386.
[38] Y. Inoue, Y. Kuroda, Y. Yamanoi, Y. Yabuki, and H. Yokoi, "Development of wrist separated exoskeleton socket of myoelectric prosthesis hand for symbrachydactyly," *Cyborg Bionic Syst.*, vol. 5, Jan. 2024, Art. no. 0141.
[39] F. Cordella, A. L. Ciancio, R. Sacchetti, A. Davalli, A. G. Cutti, E. Guglielmelli, and L. Zollo, "Literature review on needs of upper limb prosthesis users," *Frontiers Neurosci.*, vol. 10, p. 209, May 2016.
[40] T. R. Dillingham, L. E. Pezzin, E. J. MacKenzie, and A. R. Burgess, "Use and satisfaction with prosthetic devices among persons with trauma-related amputations," *Amer. J. Phys. Med. Rehabil.*, vol. 80, no. 8, pp. 563–571, Aug. 2001.



RISHI ADUSUMILLI received the B.S. degree in mechanical engineering from Coventry University, Coventry, U.K., in 2016, and the M.S. degree in mechanical engineering from the State University of New York at Buffalo, Buffalo, NY, USA, in 2020.

From 2016 to 2017, he was a Research Intern with Indian Institute of Science (IISc), Bengaluru, India. From 2019 to 2021, he was a Research Assistant with the University at Buffalo, focusing on design and analysis in mechanical engineering. Since 2021, he has been a Mechanical Design Engineer with Philips, Bothell, WA, USA, where he is part of the NPD Mechanical Engineering team for the Automated External Defibrillator (AED) product line. His research interests include designing electro-mechanical components, performing finite element analysis (FEA), and developing functional prototypes.



SOUVIK PODDAR received the B.Tech. degree in production engineering from the National Institute of Technology Agartala, India, in 2018, the M.S. degree in mechanical engineering from Arizona State University, Tempe, AZ, USA, in 2020, and the Ph.D. degree in mechanical engineering from the University at Buffalo, Buffalo, NY, USA, in 2026.

From 2018 to 2020, he was a Research Assistant with Arizona State University, where his work focused on soft robotics and the development of portable soft pneumatic exosuits for knee extension assistance in stroke rehabilitation. From 2020 to 2026, he conducted research at the University at Buffalo on cable-driven robotic prosthetic emulators and robot-resisted gait rehabilitation for individuals with cerebral palsy. From 2025 to 2026, he was a Visiting Scholar with the University of Michigan, Ann Arbor, where he conducted human-subject experiments using robotic emulators to investigate design trade-offs in transradial prostheses. His research interests include assistive and rehabilitation robotics, upper-limb prostheses, wearable robotics, biomechanics, human–robot interaction, and soft robotics.



MOHAMED SULAIMAN received the B.Tech. degree in mechanical engineering from Vellore Institute of Technology, Chennai, India, in 2019, and the M.S. degree in robotics from the University at Buffalo, Buffalo, NY, USA, in 2021.

From 2016 to 2017, he was an Engineering Intern with BorgWarner Inc., Chennai. From 2020 to 2021, he was a Graduate Research Assistant with the Assistive Wearable Robotics Laboratory, University at Buffalo, where he conducted research on deep learning-based robotic prosthetic wrist control using EMG signals. His work involved motion capture, 3-D reconstruction, and convolutional neural network applications for real-time control. Since 2022, he has been a Robotics Engineer with Hello Robot Inc., Martinez, CA, USA. His research interests include assistive robotics, mechatronics, deep learning for robotic control, and human–robot interaction. He has received multiple project awards, including the Best Project University Award from 2018 to 2019 and the IoT Challenge Winner recognition.



JIYEON KANG (Member, IEEE) received the B.S. and M.S. degrees in mechanical and aerospace engineering from Seoul National University, Seoul, South Korea, in 2008 and 2010, respectively, and the Ph.D. degree in mechanical engineering from Columbia University, New York, NY, USA, in 2018.

She was a Postdoctoral Research Fellow with the University of Michigan, in 2018. From 2019 to 2022, she was an Assistant Professor with the Department of Mechanical and Aerospace Engineering, University at Buffalo, The State University of New York. She was an affiliated Assistant Professor with the Department of Rehabilitation Science and a Research Associate with Buffalo VA Medical Center during the same period. Since 2023, she has been an Associate Professor with the AI Graduate School, Gwangju Institute of Science and Technology (GIST), Gwangju, South Korea. She has conducted clinical studies using robotic systems for patients with cerebral palsy, Parkinsons disease, and cerebellar ataxia. Her research interests include human–robot interaction, cable-actuated robotics, biomechanical data-driven control optimization, and assistive devices for individuals with special needs.